

Spin glass behavior in frustrated quantum spin system CuAl_2O_4 with a possible orbital liquid state

R. Nirmala^{1,2,3}, Kwang-Hyun Jang^{1,3}, Hasung Sim^{4,5}, Hwanbeom Cho^{4,5}, Junghwan Lee^{1,3}, Nam-Geun Yang^{1,3}, Seongsu Lee^{6,7}, R. M. Ibberson^{8,9}, K. Kakurai¹⁰, M. Matsuda^{10,11}, S.-W. Cheong⁷, V.V. Gapontsev¹² and S.V. Streltsov^{12,13} and Je-Geun Park^{1,3,4,5*}

¹*Center for Strongly Correlated Materials Research, Seoul National University, Seoul 08826, Korea*

²*Department of Physics, Indian Institute of Technology Madras, Chennai 600 036, India*

³*Department of Physics, Sungkyunkwan University, Suwon 16419 Korea*

⁴*Center for Correlated Electron Systems, Institute for Basic Science, Seoul 08826, Korea*

⁵*Department of Physics and Astronomy, Seoul National University, Seoul 08826, Korea*

⁶*Neutron Science Division, Korea Atomic Energy Research Institute, Daejeon 34057, Korea*

⁷*Rutgers Center for Emergent Materials and Department of Physics and Astronomy, Rutgers University, Piscataway, New Jersey 08854, USA*

⁸*ISIS Facility, Rutherford Appleton Laboratory, Didcot OX11 0QX, UK*

⁹*Chemical and Engineering Materials, Oak Ridge National Laboratory, Oak Ridge, Tennessee 37831, USA*

¹⁰*Quantum Beam Science Center, Japan Atomic Energy Agency, Tokai, Ibaraki 319-1195, Japan*

¹¹*Quantum Condensed Matter Division, Oak Ridge National Laboratory, Oak Ridge, Tennessee 37831, USA*

¹²*M.N. Miheev Institute of Metal Physics of Ural Branch of Russian Academy of Sciences, 620137, Ekaterinburg, Russia*

¹³*Ural Federal University, Mira St. 19, 620002 Ekaterinburg, Russia*

* Corresponding author

E-mail: jgpark10@snu.ac.kr

Abstract

CuAl_2O_4 is a normal spinel oxide having quantum spin, $S=1/2$ for Cu^{2+} . It is a rather unique feature that the Cu^{2+} ions of CuAl_2O_4 sit at a tetrahedral position, not like the usual octahedral position for many oxides. At low temperatures, it exhibits all the thermodynamic evidence of a quantum spin glass. For example, the polycrystalline CuAl_2O_4 shows a cusp centered at ~ 2 K in the low-field dc magnetization data and a clear frequency dependence in the ac magnetic susceptibility while it displays logarithmic relaxation behavior in a time dependence of the magnetization. At the same time, there is

a peak at ~ 2.3 K in the heat capacity, which shifts towards higher temperature with magnetic fields. On the other hand, there is no evidence of new superlattice peaks in the high-resolution neutron powder diffraction data when cooled from 40 to 0.4 K. This implies that there is no long-ranged magnetic order down to 0.4 K, thus confirming a spin glass-like ground state for CuAl_2O_4 . Interestingly, there is no sign of structural distortion either although Cu^{2+} is a Jahn-Teller active ion. Thus, we claim that an orbital liquid state is the most likely ground state in CuAl_2O_4 . Of further interest, it also exhibits a large frustration parameter, $f = |\theta_{\text{CW}}/T_m| \sim 67$, one of the largest values reported for spinel oxides. Our observations suggest that CuAl_2O_4 should be a rare example of a frustrated quantum spin glass with a good candidate for an orbital liquid state.

PACS numbers: 75.47.Lx, 75.50.Lk, 75.30.Cr

Introduction

A magnetic system with bond or site disorder often exhibits a short-ranged order, indicating that the system cannot form a true thermodynamic ground state and thus becomes frustrated. This state of matter, so-called spin glass, with a multitude of a ground state degeneracy has drawn considerable interest over the past few decades [1,2]. More recently, there have been intensive studies on a quantum version of the spin glass, in particular, in a lattice with Cu^{2+} ions, and a more exotic quantum spin liquid phase.

The AB_2O_4 (where A = divalent cation such as Cu, Fe and Co; B = trivalent cation such as Al and Fe) family of spinel oxides is known for their unique magnetic properties. In fact, their magnetic properties highly depend upon the cation distribution in the basic cubic structure (space group $Fd-3m$, no. 227). Often, an inversion parameter (x) defined as the amount of trivalent cations at the tetrahedral sites ($8a$) is used to identify whether a spinel oxide forms in one of either ‘largely normal’ or ‘largely inverse’ structures [3]. It is usually accepted among the community that a ‘normal spinel’ structure is formed for $0 < x < 2/3$ while an ‘inverse spinel’ structure is stabilized with $2/3 < x < 1$. While the A-site of the spinel structure forms a diamond lattice, the B-site forms a pyrochlore lattice. This pyrochlore lattice hosts a three-dimensional network of corner-sharing tetrahedra, which for antiferromagnetic interactions gives rise to intrinsic geometric frustration leading to novel emergent properties such as spin ice, cluster glass, etc. [4,5,6]. Some of spinel compounds with magnetic ions at the B-site show glassy behavior too [7,8].

On the other hand, normal spinel oxides with magnetic ions at the A-site are expected to have a collinear antiferromagnetic ground state [9]. In these oxides, A-A nearest-neighbors (NN) interaction is stronger as compared with A-B and B-B interactions.

In fact, being bipartite a diamond structure does not, a priori, have frustration with nearest-neighbor interaction alone, regardless whether it be antiferromagnetic or ferromagnetic. Nevertheless, strong magnetic frustration effects were observed in the physical properties of a few normal sulphospinels such as MnSc_2S_4 and FeSc_2S_4 [10]. This then led to an idea that these systems could be explained by a Hamiltonian including next-nearest-neighbor (NNN) antiferromagnetic exchange interaction [11]. Theoretical studies have also shown that with this NNN interaction the normal A-site spinel can exhibit various degenerate magnetic ground states [11]. It should be noted that some A-site normal spinels such as FeAl_2O_4 and CoAl_2O_4 are known to display glass-like behavior due to the competition between the NN and NNN interactions for the diamond structure of the A-sublattice [11,12,13].

Several experimental studies have so far been made to achieve a better understanding of the ground state magnetic properties of TAl_2O_4 ($\text{T} = \text{Co}, \text{Fe}$ and Mn) oxides with the normal spinel structure. For example, while CoAl_2O_4 and FeAl_2O_4 display spin glass-like ground states, FeAl_2O_4 shows a sign of an additional orbital freezing at lower temperatures. On the other hand, MnAl_2O_4 shows a long-ranged antiferromagnetic order below 40 K [13,14,15]. Among these TAl_2O_4 systems, CoAl_2O_4 is the most frustrated material lying close to a quantum critical point of an antiferromagnetic state [12,16].

By comparison, there have been relatively very few studies on the magnetic properties of copper-based normal spinel oxides and their physical properties remain largely unexplored. Naturally, the quantum spin ($S=1/2$) of Cu^{2+} makes it an attractive candidate, which might harbor an exotic quantum magnetic ground state. Therefore, it will

be interesting to examine the ground state of the Cu-based $S=1/2$ systems in detail. Of several Cu-based spinel compounds, CuGa_2O_4 is reported to have an inverse spinel structure and to exhibit a spin-glass state below 2.5 K [17, 18]. A brief report [18] was also made about the non-zero values of a zero-point entropy for both CuGa_2O_4 and CuAl_2O_4 , indicative of unusual ground state properties. We also note that nanostructured CuAl_2O_4 has been studied for possible photocatalytic applications [19]. However, to our best knowledge there is no report of the physical properties of CuAl_2O_4 .

This work focuses on the Cu-based A-site spinel oxide of CuAl_2O_4 to find glassy behavior with an extremely large frustration parameter of $f=67$. Interestingly, the frustration seems to result from the competing NN and NNN antiferromagnetic interactions supported by the underlying diamond-like structure. The spin glass order might as well be driven by small cation disorders that are difficult to remove completely in the normal spinel oxides. Of particular interest is the fact that our high-resolution neutron diffraction data do not show any sign of structural distortion down to 0.4 K although Cu^{2+} is a Jahn-Teller active ion. This implies that CuAl_2O_4 might host a possibly quantum spin glass state in the background of an orbital liquid ground state.

Experimental Details

The polycrystalline CuAl_2O_4 sample was prepared by a solid state reaction method, starting from pure CuO and Al_2O_3 (99.99% pure, Sigma-Aldrich) [20]. The samples were heated at 900° C for 9 hours with intermediate grindings and then sintered at 1020° C for 24 hours in air. We also prepared ZnAl_2O_4 under similar conditions to use it as a non-magnetic

system for the analysis of our heat capacity data. We initially checked the quality of the sample by X-ray diffraction experiments (Miniflex II, Rigaku). There were small (less than 1%) impurity of Al₂O₃. DC magnetization measurements were performed using a SQUID magnetometer (MPMS, Quantum Design, USA) in fields up to 5 T in the temperature range of 1.8 – 300 K. We also used a He³ insert of the SQUID magnetometer to measure dc magnetization data down to 0.5 K. In order to study further the frequency dependence, we measured ac susceptibility under an ac field of 0.3 mT using the SQUID magnetometer at different frequencies from 1 to 1,000 Hz in the temperature range of 1.8 – 150 K with both zero and small dc bias fields. Magnetic relaxation measurements were carried out using the SQUID magnetometer under a standard protocol: we collected the data under 5 T as a function of time after zero-field cooling (ZFC).

Heat capacity was measured by a relaxation technique from 0.5 to 300 K with a commercial system (PPMS, Quantum Design, USA). Powder neutron diffraction (ND) experiments were carried out down to 0.4 K using two neutron instruments: one is the high-resolution time-of-flight diffractometer (HRPD) at the ISIS Facility, UK and the other is a cold triple-axis spectrometer, TAS2 of JAEA, Japan operated in a two-axis mode between 1.45 and 10 K. We also made separate high-resolution X-ray diffraction measurement using a commercial machine (D8 advance, Bruker) from 300 to 40 K equipped with a low temperature cryostat: FullProf was used for structure analysis [21].

Results and Discussion

Our high-resolution neutron and X-ray powder diffraction data confirm that our CuAl₂O₄ sample forms in a ‘largely normal’ spinel structure (see Figs. 1a & 4a) with Cu²⁺ ions at

the A-site and Al^{3+} ions at the B-site (space group $Fd-3m$, No. 227). See Table 1 for the summary of the structural information. Our estimate of the lattice parameter of 8.07683 (5) Å is close to those values reported in the previous works: 8.078(1) and 8.079 Å [22, 23]: we note that Ref 18 reported a smaller value of the lattice parameter, 8.045 Å. Our full structure analysis was carried out by the joint refinement of both neutron HRPD data and HR-XRD data taken at 40 and 300 K. The final refinement data show a significant site-inversion for Cu^{2+} ions, which occupy the otherwise forbidden octahedral B-sites (see Table 1). We note that a smaller (6 ~ 8 %) amount of site inversion was reported for other polycrystalline normal spinel oxides TAl_2O_4 (T = Co, Fe and Mn) [13,14]. It is to be noted too that a similar amount (8 %) of the site inversion was recently reported for CoAl_2O_4 single crystals [16]. All these experimental results including ours indicate how much difficult it is to remove the small site inversion completely for these TAl_2O_4 systems.

In order to study the low temperature magnetic properties, we measured the dc magnetization of CuAl_2O_4 with an applied field of 5 mT down to 0.5 K (see the inset of Fig. 1b). As one can see, there is a clear cusp centered at 2 K (T_m), indicative of a magnetic phase transition. When measured under both field-cooled and zero-field-cooled conditions, the data show a clear bifurcation behavior. This is a typical sign of spin glass behavior. As we will show later, the position of this peak moves toward higher temperature with increasing frequency. Thus, the irreversible behavior in the dc magnetization can be taken as evidence of the spin glass transition occurring at low temperature for CuAl_2O_4 . At higher temperatures, the dc magnetization follows the Curie-Weiss law with the Curie-Weiss temperature of $\theta_{\text{CW}} \sim -137$ K and the effective moment value of $\sim 1.95 \mu_{\text{B}}/\text{Cu}^{2+}$ (Fig. 1b).

This estimate of the effective moment value compares very well with the theoretical spin-only value of Cu^{2+} ion ($1.73 \mu_B$). We comment that the measured θ_{CW} is extremely large compared to the cusp temperature (T_m) with $f = 67$, where the frustration parameter (f) is defined as $f = |\theta_{\text{CW}}/T_m|$. When the frustration parameter is larger than $5 \sim 10$, it is generally considered as a highly frustrated magnet [11]. Thus, it is striking that we find f as large as 67 for CuAl_2O_4 . It was previously reported that Fe-doped CuAl_2O_4 exhibits signs of a spin glass state [24].

To put the large f value for CuAl_2O_4 in perspective, it is useful to compare it with those for other Al spinel compounds: $f \sim 10 - 22$ for CoAl_2O_4 ($S = 3/2$), $f \sim 11$ for FeAl_2O_4 ($S = 2$) and $f \sim 3.6$ for MnAl_2O_4 ($S = 5/2$) [13,14]. For comparison, f is found to be only ~ 3 for another Cu spinel compound CuGa_2O_4 although it has the same quantum spin of Cu^{2+} like CuAl_2O_4 [17]. Therefore, it is expected that over the wide temperature range of $T_m \leq T \leq |\theta_{\text{CW}}|$ CuAl_2O_4 fluctuates between many low-energy configurations, evading a long-ranged order. It is also interesting to note that the f parameter appears to fall with increasing spin S value and with increasing exchange interactions for TAl_2O_4 ($T = \text{Co}, \text{Fe}$ and Mn) oxides.

Our heat capacity data measured under 0 and 9 Tesla also confirm the weak magnetic order. The C/T vs T plot shows a broad peak centered at ~ 2.3 K in zero field, consistent with the observation of a weak magnetic transition in the susceptibility (Fig. 2). This peak shifts towards higher temperature with applied magnetic fields and reaches at ~ 4 K with 9 T. This shift of the peak position with increasing magnetic field is also consistent with a spin glass nature as we will discuss shortly. In order to model the experimental observation of

the low-temperature peak, we used a Schottky model (line) in Fig. 2a with a gap value of

$$\Delta=6.5 \text{ K}: C = Nk_B \left(\frac{\Delta}{k_B T} \right)^2 \frac{e^{-\Delta/k_B T}}{\left(1 + e^{-\Delta/k_B T} \right)^2}. \text{ As one can see, the Schottky model describes the}$$

experimental data reasonably well.

Upon close inspection, the heat capacity data show a nonlinear temperature dependence below T_m with a power of ~ 2 unlike that observed in canonical spin glass systems [2]. However, we note that T^2 dependence was also found in CoAl_2O_4 [13]. A similar T^2 dependence has also been observed in other geometrically frustrated spin glass with a Kagome structure [25]. Interestingly, a fractional power law ($T^{2.33}$) dependence was theoretically predicted for a low-temperature heat capacity in a glassy state based on classical treatments of a diamond lattice Heisenberg antiferromagnet after including competing NN and NNN interactions [11].

For further quantitative analysis of the data, we obtained the magnetic part of the heat capacity, C_m , by subtracting the heat capacity of the non-magnetic analogue ZnAl_2O_4 from the experimental data of CuAl_2O_4 (Fig. 2). From the C_m/T vs T data, we estimated a magnetic entropy as a function of temperature (see Fig. 2b). According to our estimate the magnetic entropy only reaches $S=0.843 \text{ J/mol K}$ even at 20 K, which is far smaller than the theoretical maximum molar magnetic entropy value of Cu^{2+} ion, $R\ln 2 = 5.763 \text{ J/mol K}$. This difference leads us to a value of the zero-point entropy of 4.92 J/mol K , which is very close to the value reported in Ref. [18]. If we consider the orbital degeneracy of Cu^{2+} ion with t_{2g} manifold, this theoretical value should even get increased by the additional orbital entropy of $R\ln 3$. The application of magnetic field shifts most of the magnetic entropy from low to high temperatures as expected (Fig. 2). It is interesting to note that the magnetic

entropy of FeCr₂S₄ single crystal, a candidate for an orbital glass state, reaches just over 2 J/mol-K at 20 K, which is again much smaller than the theoretical value of the combined spin and orbital entropy, $R\ln 2 + R\ln 5$ [26].

The deficit of the magnetic entropy as compared with the theoretical value can be in principle interpreted in two ways. First, it implies that some significant parts of the total entropy may be released at much lower temperature or resided at zero temperature. Another equally possible scenario is that the total entropy may be recovered at much higher temperatures although we should note that we already integrated the entropy to 20 K, which is 10 times higher than the actual transition temperature. Either way, it implies strongly that the low temperature phase of CuAl₂O₄ is nontrivial.

To further examine the nature of the weak magnetic transition, we measured the ac susceptibility of CuAl₂O₄ under an ac field of 0.3 mT at different frequencies ranging from 1 Hz to 1 kHz. The real part of the ac susceptibility (Fig. 3a) demonstrates a clear frequency dependence below 2.5 K: the peak seen at 2 K for 1 Hz shifts towards higher temperatures with increasing frequency and eventually reaches at ~2.4 K for 1 kHz. This shift of the peak temperature with increasing frequency is considered as a hallmark of spin glass, as often observed in materials with magnetic frustration or competing interactions [1, 2, 27].

The magnetization vs field data of CuAl₂O₄ show a linear field dependence at 50 and 300 K (Fig. 3b). However, a S-shaped curvature develops at lower temperatures (inset in Fig. 3b). From the data measured at 0.6 K under the magnetic field of 5 T, we estimated the magnetic moment value to be $\sim 0.12 \mu_B/\text{Cu}^{2+}$ at 5 T but the magnetization never reaches a saturation. We also note that there is a small but finite non-zero isothermal remnant

magnetization (IRM) at 0.6 K. The three observations: the S-shaped magnetization, no saturation behavior, and the IRM, are consistent with the typical behavior of canonical spin glass [2] and were previously noted for other oxides too [27].

While the frequency-dependent ac susceptibility confirms the spin glass state and its nonequilibrium characteristics, we further looked for a possible slow relaxation of the magnetization at low temperatures and performed magnetic relaxation measurements on CuAl_2O_4 . For this we specifically measured the magnetization as a function of time (t), $M(t)$, and plotted the data in the inset of Fig. 3a after normalizing the data with respect to the initial magnetization at $t = 0$, i.e. $M(t)/M(0)$. For this relaxation measurement, the sample was initially zero-field-cooled to each target temperature from 300 K. After a magnetic field of 5 T was switched on and the field was stabilized ($t = 0$), we started to collect the time-dependent data. As one can see in the figure, the magnetic relaxation effects are clearly observable below 10 K; which becomes most pronounced at 2 K, coinciding with the cusp temperature in the dc and ac magnetization data (Figs. 1 & 3). The magnetization still shows relaxation behavior even after waiting for more than an hour at 2 K. Note that time was measured in seconds in the inset of Fig. 3a. The magnetic relaxation behavior is a canonical feature of spin glass [1,2,28]. We further comment that the magnetization ratio is almost linear in the $\log(t)$ plots in the glassy region: which is also a characteristic of a conventional spin glass, indicating the evolution of a broad distribution of spin relaxation rates in the vicinity of the freezing temperature [29].

Although all the bulk data discussed above consistently show that the low-temperature transition is of spin glass origin, one needs further microscopic studies such as neutron

diffraction experiment. In order to investigate the temperature evolution of the crystal as well as magnetic structures, we carried out high-resolution neutron powder diffraction experiments from 300 to 0.4 K using the HRPD beamline of the ISIS facility, UK. Our data collected at 40 K can be well fitted with the normal spinel structure as discussed above (see Table 1). Most interestingly, a direct comparison of the data with that taken at 0.4 K does not show any new superlattice peaks at the low temperatures (see the difference curve of Fig. 4b). This is clear evidence in favor of the absence of any long-ranged order in CuAl_2O_4 . We further note that a separate measurement using a triple-axis-spectrometer, TAS2 of JAEA, also produced a very similar picture, i.e. no sign of magnetic ordering in the low-temperature diffraction data, reinforcing our view that the magnetic transition seen in CuAl_2O_4 is not of a long-ranged order.

Of further interest is also the fact that our data collected both above and below the transition temperature failed to show any sign of structural distortion: all our diffraction data are consistent with the cubic $Fd-3m$ space group. This is quite surprising given the fact that Cu^{2+} is a Jahn-Teller active ion. To further demonstrate this point, we show the enlarged picture of the (4 0 0) and (2 2 2) Bragg peaks as the insets in Fig. 4b: both peaks have more or less the same value of FWHM (Full Width at Half-Maximum) at 40 and 0.4 K: for the (400) peak it is $\text{FWHM}=0.00353(4)$ at 0.4 K and $\text{FWHM}=0.00349(4)$ at 40 K; for the (222) peak it is $\text{FWHM}=0.00371(3)$ at 0.4 K and $\text{FWHM}=0.00375(3)$ at 40 K. Furthermore, we carried out high-resolution XRD experiments using a commercial machine with the resolutions of 0.04° (Bruker D8 Discover).

As a separate analysis of possible structural distortions, we simulated the diffraction patterns for the (400) and (222) peaks with a hypothetical tetragonal distortion of 0.5%

elongation along the c-axis. As one can see in the dashed-line next to the data in the inset of Fig. 4b, this rather small tetragonal distortion split the (400) peaks, which is easily detectable by our high-resolution neutron diffraction experiment. Thus we can safely put the upper bound of a possible Jahn-Teller distortion for CuAl_2O_4 at lower than 0.1%. However, it is still possible that Cu^{2+} ions undergo a local Jahn-Teller distortion without breaking the global symmetry. Local probes such as a total scattering technique might be helpful to answer this question although our high-resolution diffraction data seem to put it in doubt.

Before moving on to the theoretical discussion as to the absence of the Jahn-Teller distortion in CuAl_2O_4 , we would like to point out a subtle, but importance difference for the tetrahedral symmetry as compared to the octahedral configuration. The usual Jahn-Teller distortion of ions at the octahedral surrounding, e.g. perovskite oxides, is defined as a distance between a metal (Me) ion and oxygen (O). However, the Jahn-Teller distortions for the tetrahedra symmetry is not measured by a Me-O distance, but by a O-Me-O angle. This difference between O-Me-O angles then translates to the c/a ratio, which is the hallmark of the Jahn-Teller distortions for ions at the tetrahedral configuration. This value is usually not that small and can be easily detectable by X-ray or neutron diffractometer with reasonable resolutions: e.g. the c/a ratio is 0.91 for both CuCr_2O_4 and CuRh_2O_4 and about 1.04 for NiCr_2O_4 and NiRh_2O_4 [30]. As the measure of local distortions, we calculate two O-Me-O angles for CuRh_2O_4 , 122.6° and 103.3° , and the difference between the two angles, i.e. the strength of the local distortion for CuRh_2O_4 , is as large as 19.3° while it is zero to the accuracy of better than 0.1% for CuAl_2O_4 .

As the Cu^{2+} ion experiences the tetrahedral crystal field of neighboring four oxygen ions, it is expected to have three t_{2g} levels (d_{xy} , d_{xz} , and d_{yz}) separated from the two low-lying e_g levels ($d_{x^2-y^2}$ and d_z^2). Therefore, there is one hole in the t_{2g} manifold for CuAl_2O_4 , which is susceptible to a further Jahn-Teller distortion to lower the total energy [31]. The absence of Jahn-Teller distortion in our sample strongly suggests that a possibly orbital liquid state is being realized for CuAl_2O_4 . (See Fig. 1a for our schematic diagram for an orbital liquid-like state within the diamond structure of CuAl_2O_4). We note that for octahedral Cu^{2+} the Jahn-Teller distortion yields a low-symmetry distortion around the transition-metal ion and increases the stabilization energy [32,33,34].

In order to check this idea, we performed *ab initio* calculations within the local density approximation (LDA) and the linearized muffin-tin orbitals (LMTO) method [35]. Using the Wannier function projection procedure [36], we estimated hopping parameters between different t_{2g} orbitals. Since these orbitals are degenerate, there are no dominating elements in the hopping matrix. The Frobenius norm of the hopping matrix for nearest neighbor Cu ions $\|t\|_{nn} = 130$ meV. This results in a strong exchange coupling $J_{nn} = 4t^2/U \sim 110$ K ($U \sim 7$ eV in cuprates [37]), which should give a very large Neel temperature in a strong contrast to experimental findings. The origin of a strong suppression of the ordering temperature in CuAl_2O_4 is in a strong frustration of the exchange interaction. Indeed, our LDA calculations show that next nearest neighbor Cu, $\|t\|_{n\bar{n}} = 110$ meV, is only slightly smaller than for nearest neighbors $\|t\|_{nn} = 130$ meV. Then, the ratio between corresponding exchange constants J_2/J_1 , characterizing degree of frustration, is of order of $(\|t\|_{n\bar{n}}/\|t\|_{nn})^2 \sim 0.7$, which implies strong suppression of the ordering temperature [11] and additionally supports the possibility of the orbital liquid state in CuAl_2O_4 . This theoretical

calculation support the idea too that the combination of the NN and NNN interactions gives rise to the magnetic frustration of CuAl_2O_4 .

It is of further interest to recall that $\text{Ba}_3\text{CuSbO}_9$ having a honeycomb lattice system with Cu^{2+} ($S=1/2$) ions does not show any sign of Jahn-Teller distortion. It has thus been interpreted as another geometrically frustrated system with spin-orbital liquid properties [38,39]. We also note that as Cu^{2+} with the t_{2g} manifold is rather rare among Cu oxides CuAl_2O_4 offers a new opportunity of exploring quantum magnetism with the t_{2g} physics.

A passing comment, Cu^{2+} ions with partially filled e_g -orbitals experience the strongest Jahn-Teller distortions in octahedral surrounding. The main reason is that the e_g -orbitals are directed to ligands, oxygen in our case, whereas t_{2g} -orbitals look as much as possible away. As a result, a large difference of 0.2~0.3 Å exists between long and short bonds in compounds like LaMnO_3 and KCuF_3 while in LaTiO_3 and YTiO_3 having a single electron in t_{2g} orbitals exhibit a distortion, an order of magnitude smaller [30]. For the tetrahedral symmetry, the situation is just opposite. As a result the coupling of electronic subsystem with the lattice is weaker for Cu^{2+} in the tetrahedral configuration and the Jahn-Teller distortion are expected to be much smaller.

Last, not least, we would like to make a general comment. Unlike many Cu spin systems, including high-Tc Cu superconductors, our study on CuAl_2O_4 offers a rare case, in which Cu ions sit at a tetrahedral configuration. To our view, this difference in the local chemistry makes our studies rather unique. This tetrahedral symmetry with t_{2g} manifolds having one hole exhibits much weaker Jahn-Teller distortion simply because of the generic

wave function of t_{2g} orbitals. We believe that this point is very important to realizing the orbital liquid phase.

Summary

To summarize, a large frustration parameter is observed in the A-site magnetic spinel oxide CuAl_2O_4 , with Cu^{2+} ($S=1/2$). All the bulk measurements such as frequency-dependent ac susceptibility, magnetic relaxation behavior and specific heat indicate a spin glass transition around 2 K, consistent with the neutron diffraction data. We speculate that this spin glass order might possibly be aided by the small cation disorder in addition to the competing NN and NNN interactions. Most interestingly, our high-resolution neutron powder diffraction experiments do not show any sign of structural transition. The lack of structural distortion despite Cu^{2+} ion being Jahn-Teller active indicates that an orbital liquid state might be realized for CuAl_2O_4 . Thus, the low temperature phase of CuAl_2O_4 can be considered as a candidate for a quantum spin glass on the orbital liquid lattice.

Acknowledgements

We acknowledge D. Khomskii and Y. B. Kim for useful discussion, and the Quantum Design, Japan, for allowing us to use their He^3 option of heat capacity set-up. R.N would like to thank the IBS-CCES for support during her summer visits. Work at IIT Madras was supported by the institute NFSC and ERP schemes while work at IBS-CCES was supported by IBS-R009-G1. The work at Rutgers University was supported by the DOE under Grant No. DOE: DE-FG02-07ER46382. The work at Ekaterinburg was supported by the RFBR via 16-32-60070 program and by the FASO via theme ``Electron" No. 01201463326.

References

- [1] Murani A P, 1974 J. Phys. F: Met. Phys. **4**, [757](#)
- [2] Mydosh J A, 1993 *Spin glasses: An experimental introduction* (Taylor & Francis, London)
- [3] Nakatsuka A, Ikeda Y, Yamasaki Y, Nakayama N, Mizota T, 2003 Solid State Commun. **128**, [85](#)
- [4] Bramwell S T and Gingras M J P, 2001 Science **294**, [1495](#).
- [5] Ramirez A P, Hayashi A, Cava R J, Siddharthan R and. Shastry B S, 1999 Nature **399**, [333](#)
- [6] Lee S-H, Broholm C, Ratcliff W, Gasparovic G, Huang Q, Kim T H and Cheong S – W, 2002 Nature **418**, [856](#)
- [7] Anderson P W, 1956 Phys. Rev. **102**, [1008](#)
- [8] Jo Y, Park J-G, Kim H C, Ratcliff W and Cheong S-W, 2005 Phys. Rev. B **72**, [184421](#)
- [9] Roth W L, 1964 J. Phys. (Paris) **25**, [507](#)
- [10] Fritsch V, Hemberger J, Büttgen N, Scheidt E -W, Nidda H -A. K v, Loidl A and Tsurkan V, 2004 Phys Rev. Lett. **92**, [116401](#)
- [11] Bergman D, Alicea J, Gull E, Trebst S and Balents L, 2007 Nature Phys. **3**, [487](#)
- [12] MacDougall G J, Gout D, Zarestky J L, Ehlers G, Podlesnyak A, McGuire M A, Mandrus D and Nagler S E, 2011 PNAS **108**, [15693](#)
- [13] Tristan N, Hemberger J, Krimmel A, Nidda H -A K v, Tsurkan V and Loidl A, 2005 Phys. Rev. B **72**, [174404](#)
- [14] Suzuki T, Nagai H, Nohara M and Takagi H, 2007 J. Phys.: Condens. Matter **19**, [145265](#)

- [15] Nair H S, Fu Z, Voigt J, Su Y and Brückel T, 2014 Phys. Rev. B **89**, [174431](#)
- [16] Zaharko O, Christensen N B, Cervellino A, Tsurkan V, Maljuk A, Stuhr U, Niedermayer C, Yokaichiya F, Argyriou D N, Boehm M, and Loidl A, 2011 Phys. Rev. B **84**, [094403](#)
- [17] Petrakovskii G A, Aleksandrov K S, Bezmaternikh L N, Aplesnin S K, Roessli B, Semadeni F, Amato A, Baines C, Bartolomé J and Evangelisti M, 2001 Phys. Rev. B **63**, [184425](#)
- [18] Fenner L A, Wills A S, Bramwell S T, Dahlberg M and Schiffer P, 2009 J. Phys. Conf. Series **145**, [012029](#)
- [19] Hassanzadeh-Tabrizi S.A, Pournajaf R, Moradi-Faradonbeh A, and Sadeghinejad S, 2016 Cermics International **42**, [14121](#)
- [20] Jang K-H, 2005 MSc thesis, Sungkyunkwan University
- [21] Rodriguez-Carvajal J, 1993 Physica B **192** [55](#)
- [22] Paulsson H and Rosén E, Allg Z A 1973 Chem. **401**, [172](#)
- [23] Areán C O and Viñuela J S D, 1985 Journal of Solid State Chemistry **60** [1-5](#)
- [24] Maiti S, Kundu A K, Lebedev O I., Bera P, Anandan C, Gayen A and Seikh M M 2015 RSC Adv. **5**, [83809–83817](#)
- [25] Ramirez A P, Espinosa G P and Cooper A S, 1990 Phys. Rev. Lett. **64**, [2070](#)
- [26] Buttgen N, Hemberger J, Fritsch V, Krimmel A, Mücksch M, Krug von Nidda H-A, Lunkenheimer P, Fichtl R, Tsurkan V, and Loidl A, 2004 New Journal of Physics **6**, 191
- [27] Park J, Lee S, Park J-G, Swainson I P, Moritomo Y, Ri H-C, 2000 Phys. Rev. B **62**, [13848](#)
- [28] Binder K and Young A P, 1986 Rev. Mod. Phys. **58**, [801](#)

- [29] Park J-G, Jo Y, Park J, Kim H C, Ri H-C, Xu S, Moritomo Y, Cheong S-W, 2003 *Physica B* **328**, 90
- [30] Goodenough J B 1963 *Magnetism and the Chemical Bond* (John Wiley & Sons Ltd., London)
- [31] West A R, 2014 *Solid state chemistry and its applications* (John Wiley & Sons Ltd., London)
- [32] Ruiz-Fuertes J, Segura A, Rodri'guez F, Errandonea D, and Sanz-Ortiz M. N, 2012 *Phys. Rev. Lett.* **108**, 166402
- [33] Loa I, Adler P, Grzechnik A, Syassen K., Schwarz U, Hanfland M., Rozenberg G. Kh, Gorodetsky P, and Pasternak M. P, 2001 *Phys. Rev. Lett.* **87**, 12
- [34] Ruiz-Fuertes J, Friedrich A, Pellicer-Porres J, Errandonea D, Segura A, Morgenroth W, Haussühl E, Tu C-Y and Polian A, 2011 *Chem. Mater.* **23**, 4220–4226
- [35] Andersen O K and Jepsen O, 1984 *Phys. Rev. Lett.* **53**, 2571
- [36] Streltsov S V, Mylnikova A S, Shorikov A O, Pchelkina Z V, Khomskii D I, and Anisimov V I, 2005 *Phys. Rev. B* **71**, 245114
- [37] Liechtenstein A I, Anisimov V I, and Zaanen J, 1995 *Phys. Rev. B* **52**, 5467 and reference therein
- [38] Nakatsuji S S, Kuga K, Kimura K, Satake R, Katayama N, Nishibori E, Sawa H, Ishii R, Hagiwara M, Bridges F, Ito T U, Higemoto W, Karaki Y, Halim M, Nugroho A A, Rodriguez-Rivera J A, Green M A, and Broholm C, 2012 *Science* **336**, 559
- [39] Katayama N, Kimura K, Han Y, Nasu J, Drichko N, Nakanishi Y, Halim M, Ishiguro Y, Satake R, Nishibori E, Yoshizawa M, Nakano T, Nozue Y, Wakabayashi Y, Ishihara S, Hagiwara M, Sawa H, and Nakatsuji S, 2015 *PNAS* **112**, 9305

Figure Captions

Fig.1 (Color online) (a) The spinel crystal structure and a schematic diagram of t_{2g} orbitals showing the random distribution of Cu^{2+} d -states within the diamond structure of CuAl_2O_4 . (b) Inverse susceptibility vs temperature of CuAl_2O_4 taken with an applied field of 0.1 T: the Curie-Weiss fit (line) with the Curie-Weiss temperature (θ_{CW}) of -137 K and the effective moment of $1.95 \mu_{\text{B}}/\text{Cu}^{2+}$. Inset in (b) depicts the magnetization data collected down to 0.6 K after both field-cooling and zero-field-cooling using a He^3 insert of the SQUID magnetometer.

Fig. 2 (Color online) (a) Plot of C/T vs T of CuAl_2O_4 measured under applied fields of 0 and 9 T together with data (bottom) taken for ZnAl_2O_4 . The inset shows the T^2 dependence of low temperature heat capacity data with lines as guide for eyes. We used a Schottky model (line) in order to model the experimental observation of the low-temperature peak. See the text. (b) It shows the temperature dependence of the magnetic entropy.

Fig. 3 (Color online) (a) Real part of ac susceptibility (χ') vs temperature at different frequencies taken with an applied field of 0.3 mT. The arrow indicates the direction of increasing frequency. The inset shows the relaxation behavior of magnetization ratio $M(t)/M(0)$ as a function of time taken at a few selected temperatures under applied field of 5 T. (b) Magnetization vs field data of CuAl_2O_4 at a few representative temperatures: 300, 50, 2, and 0.6 K, in applied fields up to 5 T with the inset showing the low field region of the 0.6 K data.

Fig. 4 (Color online) (a) Neutron powder diffraction data of CuAl_2O_4 taken at 40 K. The symbols represent the data points with the line displaying the refinement results. The vertical ticks indicate the position of expected Bragg peaks with the difference curve shown at the bottom. (b) The difference curve between the neutron diffraction data obtained at 0.4 and 40 K shows no sign of any new superlattice peaks of magnetic origin. The insets in Fig. 4b are the enlarged pictures of the (4 0 0) and (2 2 2) Bragg peaks with similar values of FWHM, demonstrating that there is no structural distortion. We also simulated the diffraction patterns for (400) and (222) peaks for a hypothetical tetragonal distortion of 0.5% elongation along the c-axis (see the line in the inset).

Figure 1

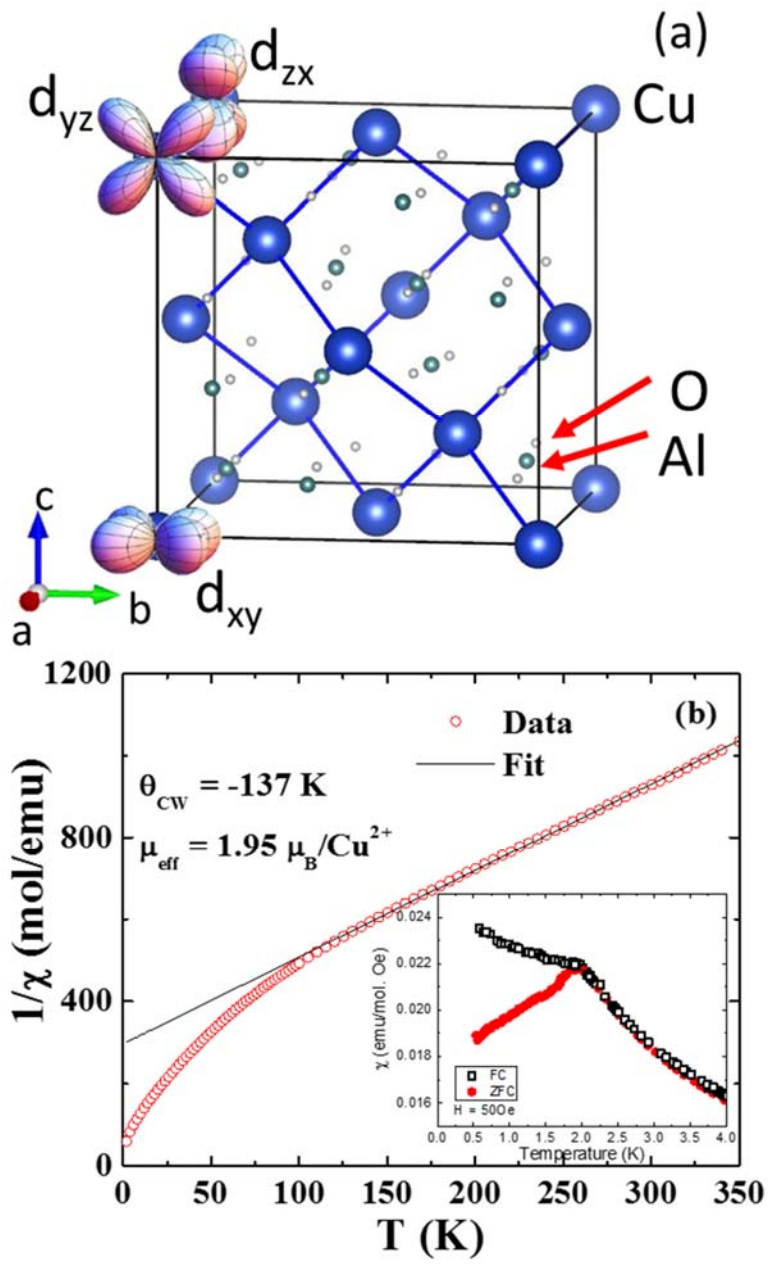


Figure 2

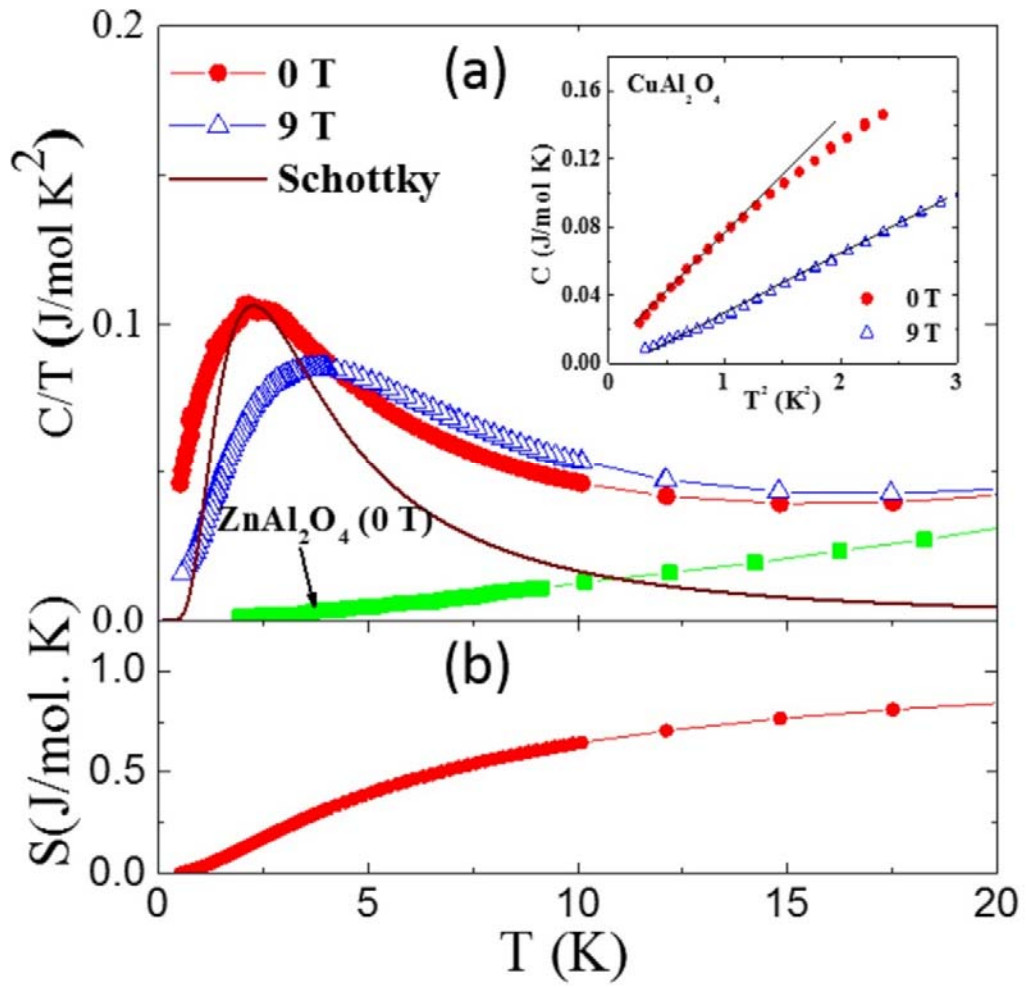


Figure 3

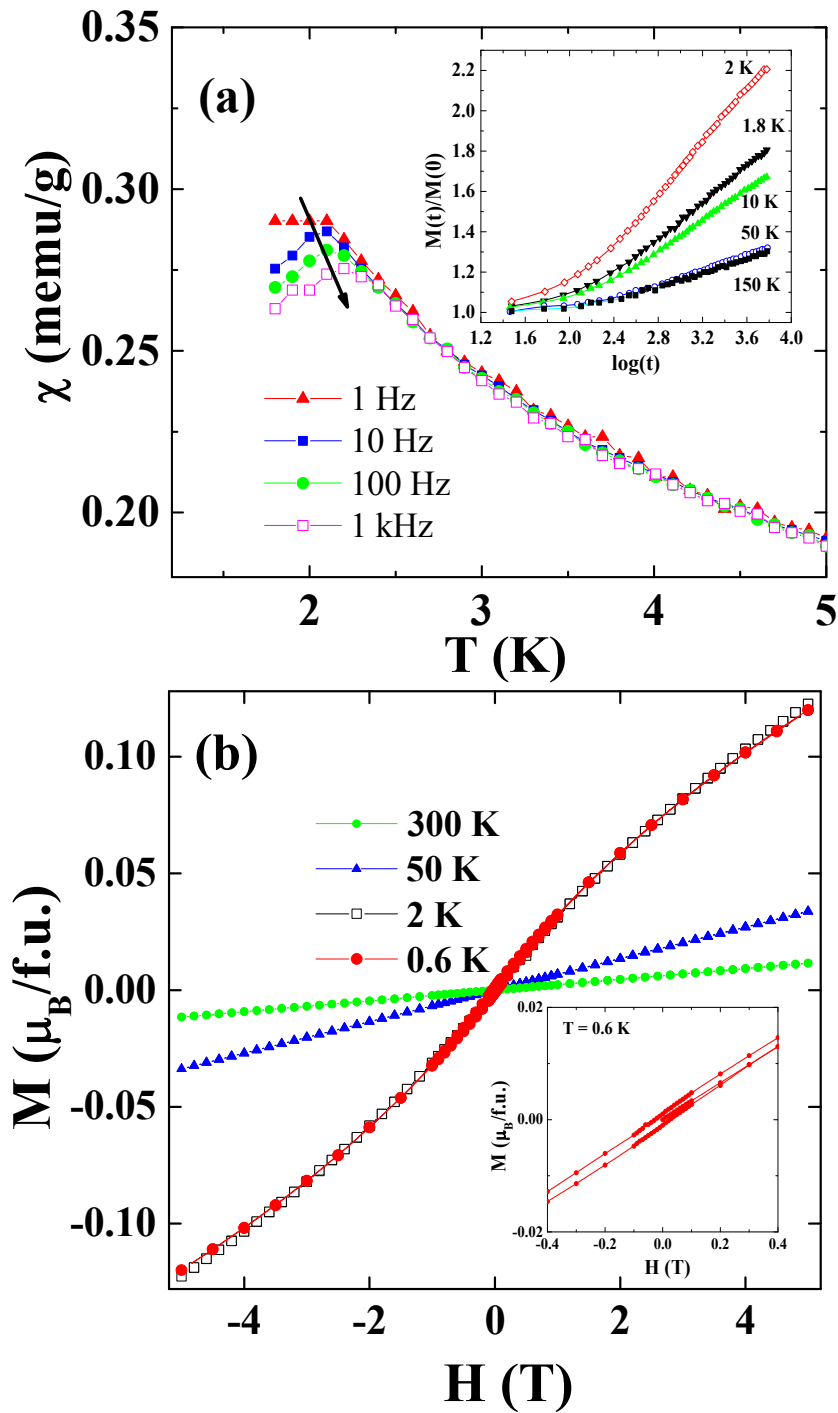


Figure 4

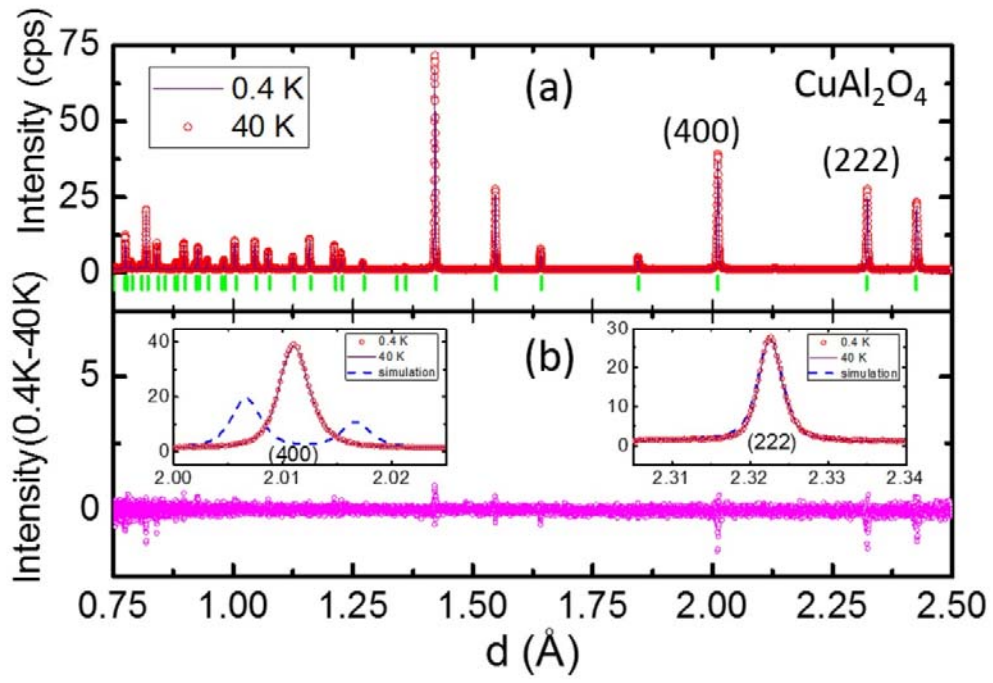


Table 1 Summary of the structural information. Bond distance at 40 K are as follows: Cu-Cu 3.494335(7); Cu-O 1.9104(6); Al-O 1.9278(6) Å. The position (0, 0, 0) are in tetrahedral sites and (5/8, 5/8, 5/8) are in octahedral site. In our final refinement, we achieved the following goodness of agreements: $R_p=8.54$, $R_{wp}=9.62$, $R_{exp}=4.43$, and $\chi^2=4.71$.

300 K	F d -3 m origin choice 1, a = b = c = 8.07683(10) Å				
	x	y	z	B	Occ
Cu	0	0	0	1.105(159)	0.029
Al	0	0	0	1.105 (159)	0.013
Al	0.625	0.625	0.625	0.505(155)	0.070
Cu	0.625	0.625	0.625	0.505(155)	0.013
O	0.38622(104)	0.38622(104)	0.38622(104)	1.056(301)	0.167

40 K	F d -3 m origin choice 1, a = b = c = 8.06983(3) Å				
	x	y	z	B	Occ
Cu	0	0	0	0.779(27)	0.029
Al	0	0	0	0.779(27)	0.013
Al	0.625	0.625	0.625	0.693(27)	0.070
Cu	0.625	0.625	0.625	0.693(27)	0.013
O	0.38645(5)	0.38645(5)	0.38465(5)	0.131(18)	0.167